Domain Structure and Interphase Dimensions in Poly(urethaneurea) Elastomers Using DSC and SAXS

S. G. MUSSELMAN,[1] T. M. SANTOSUSSO,[1] J. D. BARNES,[2] L. H. SPERLING[3]

[1] Air Products and Chemicals, Inc., Allentown, Pennsylvania 18195

[2] NIST Polymer Structure and Mechanics Group, Gaithersburg, Maryland 20899

[3] Lehigh University, Bethlehem, Pennsylvania 18015

ABSTRACT: Small-angle X-ray scattering (SAXS) and differential scattering calorimetry (DSC) were used to demonstrate distinct differences in domain size, phase separation, and hydrogen bonding in a series of segmented urethaneurea elastomers prepared from isocyanate-terminated prepolymers and aromatic diamine chain extenders. Two types of prepolymers were studied. The first contained a broadly polydisperse high molecular mass oligomer with relatively high levels of free isocyanate monomer. The second type of prepolymer contained low levels of high molecular mass oligomers with mass fractions greater than 90% of the two-to-one adduct of toluene diisocyanate (TDI) to polytetramethylene glycol (PTMEG). The mass fraction of the residual unreacted diisocyanate was less than 0.1% in the second type. Two chain extenders, 4,4'-methylene *bis*-(2-chloroaniline)(Mboca) and 4,4'-methylene *bis*-(3-chloro-2,6-diethylaniline) (MCDEA), were used to convert the prepolymers to poly(urethaneurea) elastomers. Materials prepared from the prepolymers with low oligomer polydispersity exhibited smaller hard segment domains with more ordered morphology, greater phase separation, and more hydrogen bonding than those prepared from prepolymers with high oligomer polydispersity. These tendencies were enhanced in those elastomers prepared by chain extension with MCDEA compared to those made with Mboca. © 1999 John Wiley & Sons, Inc. J Polym Sci B: Polym Phys 37: 2586–2600, 1999

Keywords: small-angle scattering; differential scanning calorimetry; microstructure; urethaneurea; elastomer

INTRODUCTION

The term polyurethane elastomer is commonly used to describe both poly(urethaneurea) and polyurethane elastomers because they share many physical and mechanical characteristics.[1] The properties of polyurethane elastomers depend on the phase separated block structure created by the rubbery soft blocks and the glassy hard blocks. The soft block is generally composed of urethane segments derived from polyether or polyester diols ranging in molecular mass from 500 g/mol to 5000 g/mol, while the hard block is usually composed of the reaction products of diisocyanates with a chain extender or crosslinker. In poly(urethaneurea) elastomers, the chain extender is usually an aromatic diamine, while a low molecular mass diol is utilized in polyurethane elastomers. In thermoset polyurethane or poly(urethaneurea) elastomers, the hard domain often contains chemical crosslinks from allophonate or biuret formation as well as so-called physical crosslinks derived from phase separation, hydrogen bonding, and/or crystallinity.

This study attempted to determine whether morphological characteristics extracted from SAXS and DSC experiments could be correlated with reported improvements in physical and mechanical properties of polyurethane elastomers[2,3] prepared from a relatively new class of prepolymers.[4]

Thermoset polyurethane elastomers are often prepared in a two-step process. First, a prepolymer is formed by the reaction of the high molecular mass diol with the diisocyanate to form an isocyanate-terminated polyurethane prepolymer. In the second step, the prepolymer in the molten state is mixed with a diamine or diol for chain extension and crosslinking.

The conventional synthesis of the prepolymer involves adding a stoichiometric excess (usually 2:1) of diisocyanate to polyol. The desired product is the 2:1 adduct of isocyanate to the polyol. However, this 2:1 ratio of isocyanate to polyol results in the formation of a statistical distribution of isocyanate functional species, which includes high molecular mass oligomers where the diisocyanate reacts with two polyols. Significant residual diisocyanate monomer remains when reaction is complete. Because of the high molecular mass oligomers, the prepolymers are quite viscous and, for practical commercial handling and processing, the residual diisocyanate monomer is left in the prepolymer as a reactive diluent to lower the viscosity. Unfortunately, this is not desirable from the viewpoint of end user health and safety because exposure to diisocyanate monomer can result in respiratory sensitization. The prepolymers prepared by this method will be referred to as statistical prepolymers.

The present process uses a large excess of the diisocyanate to control the formation of high molecular mass oligomer; therefore, the residual monomer is no longer needed to reduce viscosity and can be distilled off to a mass fraction of less than 0.1% (Fig. 1).[4] The prepolymer resulting from this process has lower polydispersity as well as a reduced potential for hazard during handling because of the reduced concentration of diisocyanate monomer. These are described as "regular" prepolymers in later sections of this paper.

Improvements in the physical and mechanical properties of elastomers chain extended with 4,4′-methylene *bis*-(2-chloroaniline) (Mboca) have been reported[2,3] when using this method to control the molecular mass distribution of TDI terminated prepolymers. It is suspected that differences in the morphology of the elastomers due to
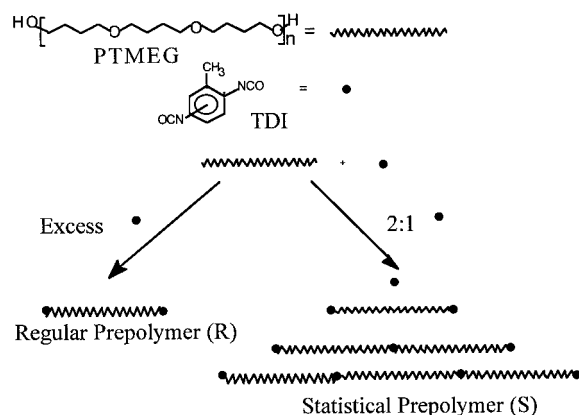

Figure 1. Prepolymer synthesis to produce a regular prepolymer (*R*) and a statistical prepolymer (*S*). The excess isocyanate of the regular prepolymer is distilled off to less than 0.1% free monomer.

the more regular structure of the prepolymer are a likely cause of the improved properties. The use of 4,4′-methylene *bis*-(3-chloro-2,6-diethylaniline) (MCDEA) as a chain extender was shown to result in further improvements in physical and mechanical properties in these types of elastomers. The properties were further optimized by use of an extended cure time and higher cure temperature.[5]

There has been a great deal of work examining the morphology of both thermoplastic and thermoset polyurethane elastomers.[6] Koberstein and co-workers[7–9] investigated domain size and the diffuse boundary thickness of crosslinked polyurethanes using small-angle X-ray scattering (SAXS). More recently, Koberstein et al.[10–13] investigated the kinetics and thermodynamics of crystallization and phase separation using differential scanning calorimetry (DSC) in addition to SAXS. The effects of variations in soft or hard segment length and type[14–20] and differences in diisocyanates[21–24] on the morphology of polyurethanes have been investigated using a variety of techniques including SAXS, DSC, dynamic mechanical thermal analysis (DMTA), wide-angle X-ray diffraction (WAXD), Fourier transform infrared spectroscopy (FTIR), and tensile testing.

The present study compared prepolymers produced with a broad oligomer polydispersity and those produced with controlled, narrow oligomer polydispersity to determine if differences in tensile, compression, and thermal properties were correlated with differences in morphology. The prepolymers were made from polytetramethylene glycol (PTMEG) and TDI (pure 2,4 TDI and iso-
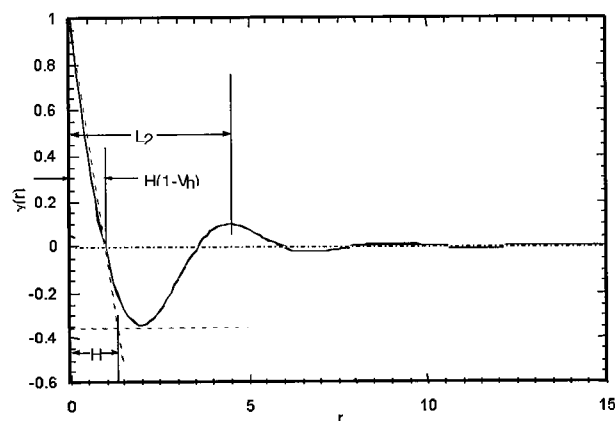
Figure 2. Schematic representation of parameters extracted from correlation function analysis.

mer mixture of 2,4/2,6 TDI) with Mboca and MCDEA as chain extenders. Differences in the interdomain spacing, size of the phases, volume fraction of the phases, and sharpness and amount of interphase were characterized by SAXS. DSC analysis was used to determine the thermal properties of the elastomers, the purity of the phases, the volume fraction of each phase and differences in the hydrogen bonding of the hard domain.

SAXS DATA TREATMENT

SAXS provides quantitative and qualitative information on the morphology of a two-phase system when the domain sizes are on the order of nanometers and the electron densities of the two phases differ sufficiently.[25–30] Under the assumption of a lamellar microstructure, and given the limited q range of the measurements, the graphical correlation function approach pioneered by Strobl and Schneider[30] was chosen to analyze the SAXS data presented here.

The method relies on applying a numerical Fourier transform to the scattering data to produce the function

$$\gamma(r) = \frac{\int_0^\infty q^2 I_L(q)\cos(qr)\,dq}{\int_0^\infty q^2 I_L(q)\,dq} \tag{1}$$

where the notation $I_L(q)$ specifically refers to the scattered intensity arising from the lamellar microstructure. This must be separated from the total observed scattering (i.e.,

$$I_{\text{obs}}(q) = I_L(q) + I_{\text{bkg}}(q) \tag{2}$$

where "obs" designates the experimental function, L designates the lamellar scattering, and "bkg" stands for "background." In the present work, the background contribution is assumed to be a constant, independent of q, arising from liquid-like density fluctuations. The method used to estimate the background contribution is described below. The scattering vector, q, is defined as

$$q = \frac{4\pi \sin\theta}{\lambda} \tag{3}$$

where θ is one half of the scattering angle and λ is the wavelength of the radiation. With reference to Figure 2, the function $\gamma(r)$ can be interpreted as the average degree of contrast between the scattering length densities at two ends of a rod of length r where the average is taken over all possible starting points for the rod within the volume of the material (Fig. 3). For small values of r, it is most likely that the two ends of the rod are in the same environment, hence the value of 1 for $\gamma(0)$. The likelihood that the two ends of the rod are in contrasting environments increases as r increases, which drives $\gamma(r)$ toward negative values. In quasi-periodic microstructures like the ones
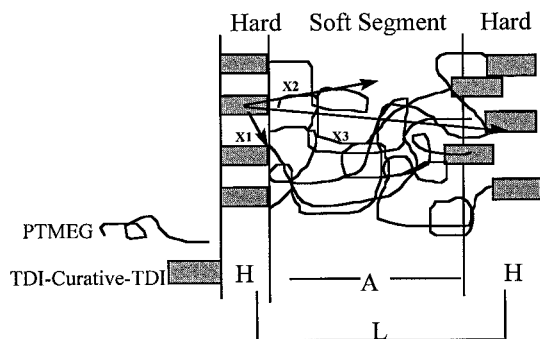

Figure 3. Lamellar structure: L is the interdomain spacing, H is the hard segment thickness, and A is the soft segment thickness. If all of the hard segments were organized ideally, the left side of the diagram would model the lamellae. Real systems with phase mixing more nearly resemble the right side.
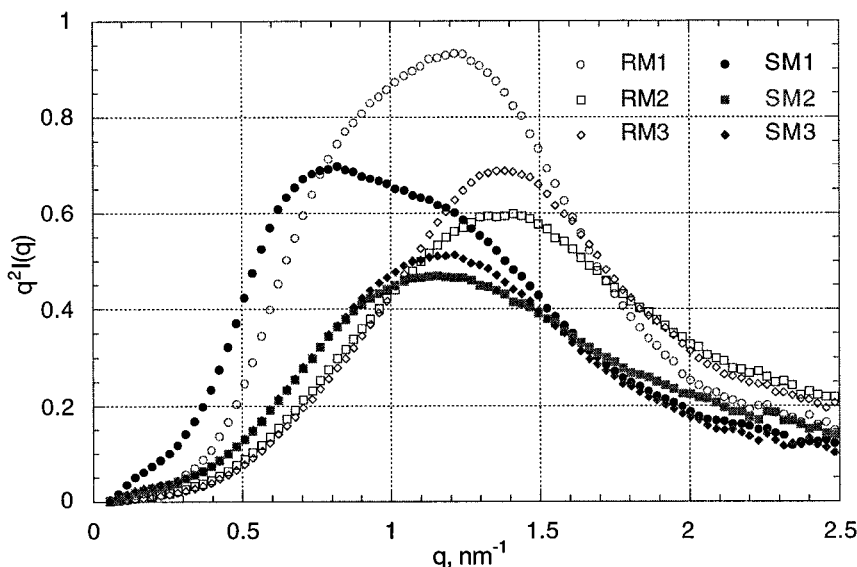
Figure 4. Plots of $I(q) q^2$ vs. q for determination of the interlamellar Bragg spacing. Error bars (see text) for the data in these plots are approximately the size of the labels for the data points.

being considered here, the degree of similarity increases again as r becomes comparable to the spacing between similar elements. As r becomes very large the correlation between the contrast at the ends of the rod vanishes, which leads to a limiting value of zero for $\gamma(r)$.

In order to carry out the integration in eq. (1), one must recall that the experimental data are necessarily truncated by the beam stop at low scattering angles and by the boundary of the detector's image area at high angles. Extrapolation functions must be provided for the data in the low q and high q ranges in order to avoid truncation effects when carrying out the integration.

The estimate for the background contribution used in this work uses the procedure of Bonart and Miller,[32] in which the slope of $q^4 I_{obs}(q)$ plotted vs. q^4 at large q is measured as an estimator for I_{bkg}, which is treated as a constant.

Once this constant background is accounted for, Porod's Law,[31,32]

$$\lim_{q \to \infty} I_L(q) = \frac{K_p}{q^4} \qquad (4)$$

is used as an extrapolating function to extend the data to high q. The extrapolating function for low q is $-(R_g/q)^2$, which is to be interpreted as a strictly empirical function with no significance ascribed to the parameter values.

The correlation function analysis therefore consists of four parts: (1) estimating the background contributions, (2) determining proper extrapolating functions for the lamellar scattering, (3) integrating over the lamellar component of the scattering, and (4) graphically assigning values to the characteristic features of the resulting correlation function. An example is shown in Figure 2.

The experience of other workers[33–36] in applying this method to similar data demonstrates that the parameters extracted in this way are suitable for interpreting differences between related materials. There are, however, no standard methods for assessing either the precision or the accuracy of the extracted values.

The procedures used to extract the parameters used in the discussion of the SAXS results discussed later in this paper are as follows. In analogy with Bragg's law the interdomain spacing, sometimes called the "long period" (L in Fig. 3), is obtained from

$$L_1 = 2\pi/q_{max}, \qquad (5)$$

where q_{max} denotes the value of q at the peak of the $I(q)q^2$ vs. q plot (Fig. 4). With reference to the example correlation function plot in Figure 2, L_2 denotes the position of the first peak maximum following the minimum in the correlation function and represents another estimator for the long
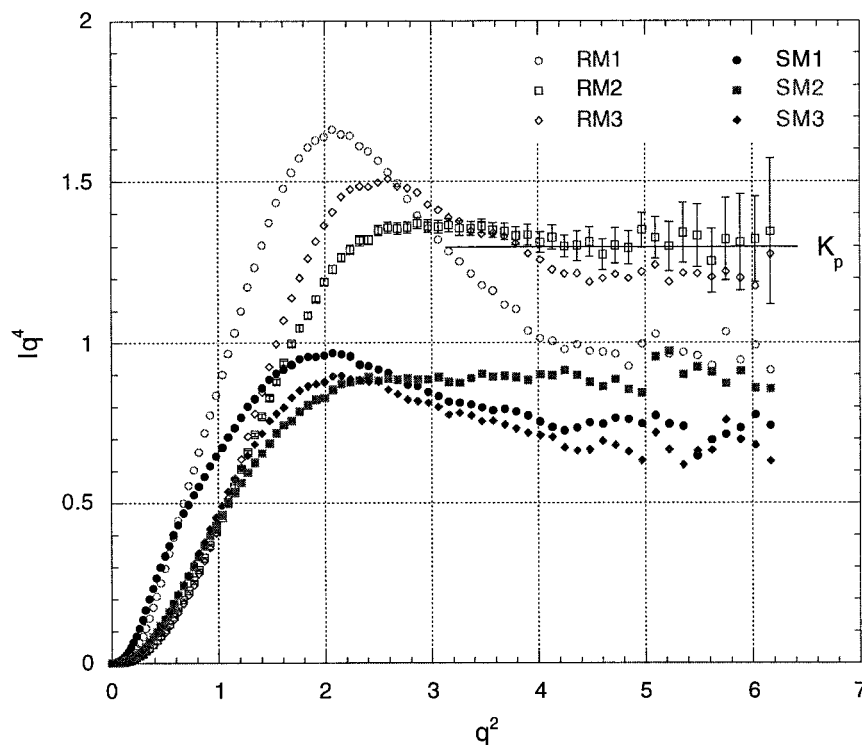
Figure 5. Porod law behavior for selected datasets. See text for description of meaning of error bars.

period. The value of r at the first zero (r_0) in $\gamma(r)$ is defined to be $H(1-V_h)$, where H is the thickness of the hard domain and V_h is the volume fraction of hard domains. H is the length of the base of the right triangle whose hypotenuse passes through $\gamma = 1$ and $\gamma = 0$ and whose base line is tangent to the $\gamma(r)$ curve at its minimum. The significance of the curvature in $\gamma(r)$ in the range $0 < r < H(1-V_h)$ remains unclear at this time. Combining the results for r_0 and H yields $V_h = 1 - (r_0/H)$. The soft domain thickness is H-L_2. Finally, K_p is obtained by inspecting the Porod plot for each data set to locate its high q asymptote (an example is shown in Fig. 5).
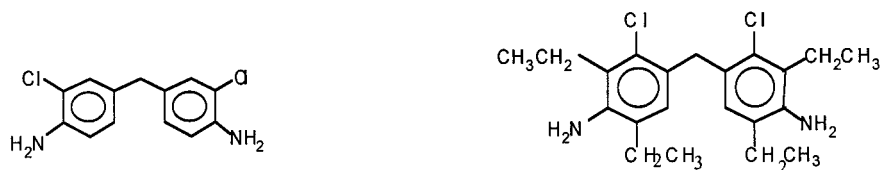
EXPERIMENTAL

Prepolymer Synthesis

Altogether 12 different kinds of polyurethanes were prepared. The reagents and curing conditions are summarized in Table I.

Four prepolymers were synthesized. Commercial 2,4 TDI, 80/20 2,4/2,6 TDI isomer mixtures (Olin[37]) and 2,4/2,6 TDI isomer mixtures (APCI) were used with PTMEG 1000 molecular mass polyol (Dupont Terathanes). The degassed polyol was added to the TDI in a reactor.

Two of the prepolymers used a TDI to polyol ratio of 2:1 to produce a statistical prepolymer (S)

Table I.   Specimen Preparation Conditions

Prepolymer	Ratio of 2,4/2,6 TDI	Mboca (100°C, 16 h)	MCDEA (100°C, 16 h)	MCDEA (130°C, 48 h)
Statistical	80/20	SM1	SM2	SM3
Statistical	100/0	SP1	SP2	SP3
Regular	80/20	RM1	RM2	RM3
Regular	100/0	RP1	RP2	RP3

4,4'-Methylene Bis-(2-Chloroaniline)   4,4'-Methylene Bis (3-Chloro-2,6-Diethylaniline)
(Mboca)   (MCDEA)

Figure 6.   Molecular structures of curatives Mboca and MCDEA.

containing mass fractions of approximately 60% high molecular mass oligomers and 2–3% residual isocyanate. Pure 2,4 TDI was used to produce one S prepolymer ($S(2,4)$) while an 80/20 TDI isomer mixture was used for the other ($S(2,4/2,6)$). The other two prepolymers were synthesized with an excess TDI to polyol ratio of 8:1 to produce a more regular (R) prepolymer containing less than 10% high molecular mass oligomer. The residual isocyanate monomer was removed by a wiped film distillation technique[4] to a mass fraction of less than 0.1%. One R prepolymer contained pure 2,4 TDI ($R(2,4)$) while the other was made with a TDI isomer mixture which, after reaction and distillation, results in an 80/20 2,4/2,6 TDI incorporation into the prepolymer ($R(2,4/2,6)$).[4] The chemical differences between these species are depicted schematically in Figure 1.

Elastomer Preparation

Twelve elastomers were prepared from the four prepolymers using hand-casting techniques. Two different curatives or chain extenders were used, 4,4'-methylene *bis*-(2-chloroaniline) (Mboca) and 4,4'-methylene *bis*-(3-chloro-2,6-diethylaniline (MCDEA) (see Fig. 6). An additional set of four MCDEA cured elastomers was subjected to a longer curing time.

The prepolymers were stored at all times under a dry nitrogen blanket. The prepolymer was heated to 70°C and degassed under vacuum. The nitrogen was reapplied and the prepolymer reheated to 70°C. Prepolymer $S(2,4/2,6)$ was heated to 90°C for processing with Mboca due to problems with crystallization of the Mboca with the residual 2,6 TDI. For processing the curatives (chain extenders) in the melt, the solid Mboca was heated to 120°C and the MCDEA was heated to 100°C. The prepolymer was present in 5% stoichiometric excess in order to allow formation of a

mole fraction of 5% biuret for chemical crosslinking. After mixing well with a spatula, the formulation was again degassed under vacuum. The formulations were poured into heated (30 × 30 × 0.16) cm and (10 × 10 × 1.3) cm glass molds with steel spacers. The molds and spacers were sprayed with a silicone-based mold release (George Mann Formulated Products). For the Mboca formulations and one set of the MCDEA formulations, the molds were at 100°C and the elastomers were cured for 16 h at 100°C. For the other set of MCDEA formulations, the molds were at 130°C and cured for 48 h at 130°C.

The resulting Mboca cured elastomers contain mass fractions of 39% TDI-Mboca-TDI triad hard segments and 61% PTMEG soft segments. The MCDEA elastomers contain mass fractions of 43% TDI-MCDEA-TDI triad hard segments and 57% soft segment.

Physical Characterization

All elastomers were aged 2 weeks at 23°C and 50% relative humidity before testing. Tensile testing following ASTM D412-92[37] utilized an Instron model 1122 mechanical tester. An XL extensometer was used with a 2.5-cm gage, and Instron grip to grip distance was 6.35 cm. Dumbbell-shaped samples were pressed from the 0.16-cm thick castings using Die C. Samples were tested at a crosshead speed of 51 cm/min. Hardness was measured following ASTM D2240[37] using Shore Durometers type D on 1.3-cm thick samples. Compression set was measured following ASTM D395 Method B.[38] Cylinders with a 2.5-cm diameter were cut from the 1.3-cm casting and then compressed 25% for 22 h at 70°C. The samples were allowed to recover for 0.5 h and the percent of compression that did not recover was reported.

DSC

Differential scanning calorimetry (DSC) was run on a TA Instruments MDSC 2929 with Thermal Analyst 3200 Software for data analysis. The samples were cooled below $-130°C$ with liquid nitrogen and ramped 10°C/min to 250°C for Mboca samples and 300°C for the MCDEA samples. For modulated testing, the modulation was ± 1°C/min and the ramp rate was 5°C/min.

SAXS

The data for this study were collected using the NIST Digital SAXS Camera, which is an adaptation of the camera built by Hendricks at Oak Ridge National laboratory.[39] It uses a multiwire gas proportional area detector to capture a two-dimensional image of the SAXS pattern. The X-rays are monochromatic Cu K$_\alpha$ ($\lambda =$ 0.154 nm) radiation from a graphite monochromator attached to a 12 kW rotating anode X-ray generator. Pinhole collimation provides a beam divergence of approximately 1 mrad. The collimation and detector paths are evacuated, with Kapton windows for the specimen chamber. The specimen to detector distance for these experiments was chosen to be approximately 3 m, yielding scattering vectors in the range $0.1 < q < 2.5$ nm^{-1}.

Computer controls provide data collection in a batch mode according to a user-specified experimental design. Samples for three of the 12 preparation conditions were replicated to check the repeatability of the SAXS measurements, giving a total of 15 samples. The experimental design used to collect the SAXS data used here comprised four series, each consisting of data collection steps from the 15 elastomer samples, an empty beam, and a secondary standard sample. Data from the four series were pooled for each specimen. This procedure helps to average out the effects of instrumental drifts, thus facilitating comparisons of data on all specimens in the series.

The transmission coefficients of the specimens were measured directly by strongly attenuating the X-ray beam, moving the primary beam away from the beam stop, and determining the ratio between the intensity of the direct beam with a specimen in place to the intensity measured with no specimen in the beam.

The measured values of the transmission coefficients were then used to correct for the contributions from the unscattered primary beam and the detector dark current. Scattering data from the secondary standard, the transmission coefficients, and the measured sample thickness were then combined to scale the data to absolute intensity units.

It was observed that all specimens in these experiments scattered isotropically, so that all of the available information from the scattering experiment can be summarized by carrying out a circular average over the detector image using an appropriate value for the beam center.

RESULTS

The samples of poly(urethaneurea) prepared above were subjected to both basic physical and mechanical studies, as well as the more intensive DSC and SAXS studies. Because the differences between the elastomers prepared with pure 2,4 TDI and those prepared with the 2,4/2,6 isomer mixture were generally minor the discussion of the scattering data focuses on the elastomers prepared with the 2,4/2,6 TDI mixtures.

Mechanical Properties

The results from tests on the mechanical properties are shown in Table II. The standard deviations given in the last row of the table are derived using the procedures specified in the respective ASTM methods. The Shore D hardness of the MCDEA elastomers is about 6–7 points harder than that of the Mboca elastomers. The rebound is higher for the MCDEA elastomer series compared to the Mboca series. The R prepolymer elastomers exhibit a small increase in rebound compared to the elastomers from the S prepolymers, this difference being more prominent for the Mboca elastomers.

The compression set shows the ability of the elastomer to recover after being compressed at high temperature. The lower the value the better the recovery or elasticity of the elastomer. The Mboca elastomer series has lower compression set than the MCDEA elastomer series. For the MCDEA elastomers, the increased cure time and temperature show an improvement in compression set.

The tensile "modulus" (stress at particular strain) values for the elastomers from the R prepolymers are higher than those of the elastomers from the S prepolymers. The MCDEA elastomer series has higher tensile modulus than the Mboca cured elastomers.

Table II.   Summary of Results from Physical Testing

ID (Table I)	Hardness Shore D	Compression Set (%)	100% Modulus (MPa)	300% Modulus (MPa)	Ultimate Tensile (MPa)	Tensile Elongation (%)	Bashore Rebound (%)
SM1	50	24	14	28	43	371	49
SP1	51	28	14	31	46	356	48
RM1	51	26	16	35	45	337	53
RP1	53	31	15	35	51	353	51
SM2	57	41	15	38	53	362	57
SP2	57	39	17	38	48	347	57
RM2	58	37	18	53	66	337	58
RP2	59	40	18	53	65	332	58
SM3	57	29	16	41	74	408	57
SP3	57	30	17	38	60	380	58
RM3	57	34	17	44	66	375	58
RP3	58	37	17	41	67	394	58
SD (see text)	2	2	0.1	0.8	1.2	4.4	1

DSC

The DSC data displayed in Table III shows that the glass-transition temperatures (T_g) of all of the Mboca cured elastomer series are the same at about $-55°C$. For the MCDEA elastomer series there was also no effect from the variation in the prepolymer, with the T_g averaging $-65°C$. Also, the additional cure at high temperatures did not affect the T_g for the MCDEA elastomers. The consistency of the T_g within a curative series indicates that the percent of phase separation is the same for all the elastomers within each curative series.

The T_g for the MCDEA cured elastomers was consistently 10°C lower than the Mboca cured elastomers (Fig. 7). A shift in glass-transition temperature is indicative of differences in the phase mixing. The greater the amount of hard segment dissolved in the soft domains the higher the expected glass-transition temperature of the soft domains. Since the composition of the soft segment is very similar to that of the Mboca elas-

Table III.   Summary of DSC Results—Thermal Property and Heat of Dissociation $(H_d)^a$

Sample ID (Table I)	H_d (J/g Elastomer)[b]	H_d (kJ/mol Hard Segment)[c]	T_g Soft Segment (°C)
SM1	11	17	−55
SP1	13	21	−57
RM1	30	47	−55
RP1	31	49	−58
SM2	9	15	−63
SP2	17	29	−68
RM2	25	42	−67
RP2	35	59	−64
SM3	16	27	−64
SP3	20	34	−65
RM3	34	57	−65
RP3	36	61	−62

[a] Non-NIST data, uncertainties not specified.
[b] Heat of dissociation for the entire mass.
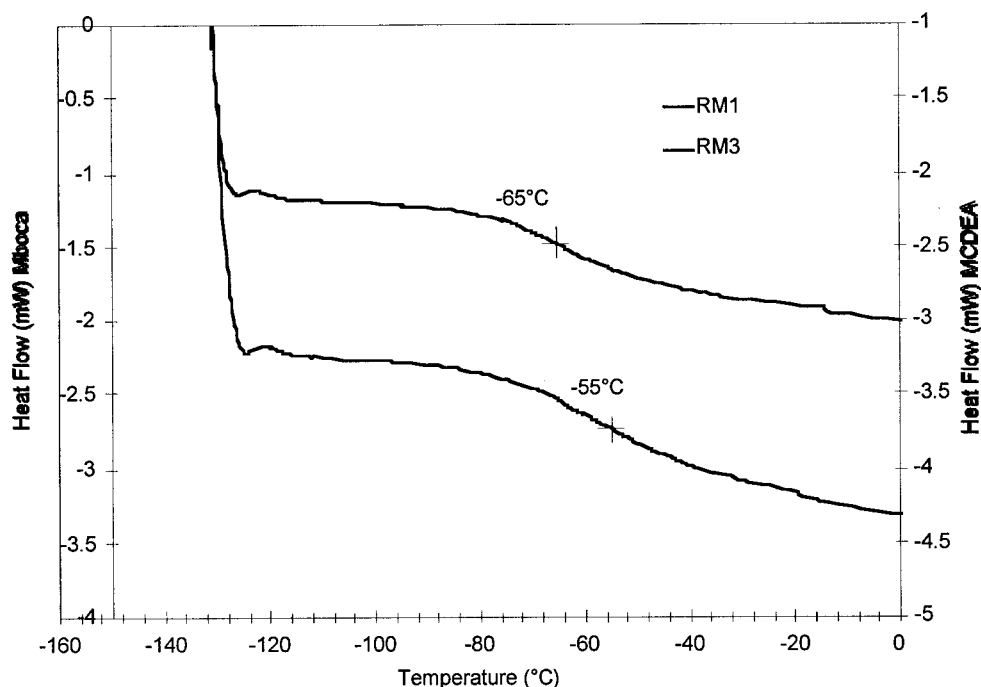[c] Heat of dissociation based on mass fraction of hard segment in elastomer.

Figure 7. DSC scans of representative Mboca and MCDEA elastomers showing a 10°C difference in soft phase low temperature T_g (see Table III).

tomers, the lower T_g indicates that the purity of the soft segment is greater for the MCDEA systems.

When comparing samples in the high temperature region (Fig. 8), it can be seen that the heat

of dissociation for the R prepolymers is two to three times greater than the S prepolymers for both the Mboca and the MCDEA elastomers. The heats of dissociation in Table III are corrected for the percent of hard segment in the elastomer to
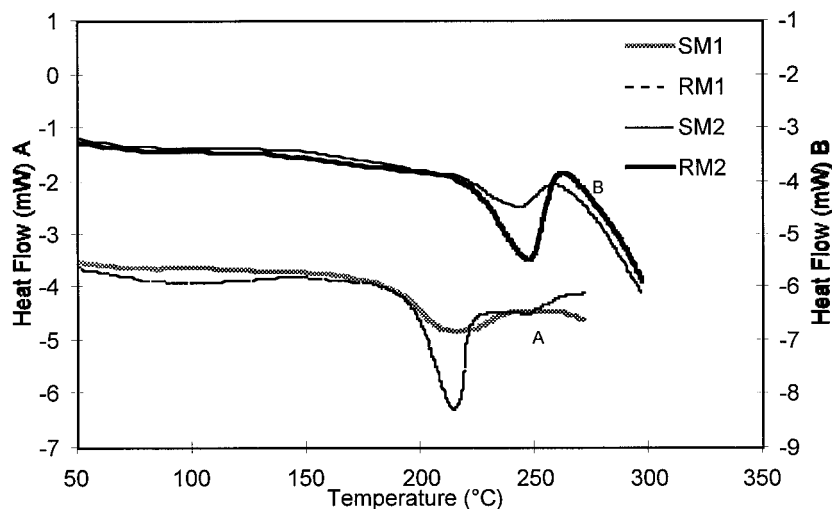

Figure 8. (A) Comparison of the heat of dissociation of an elastomer from a S prepolymer to a R prepolymer cured with Mboca. (B) Cured with MCDEA for 16 h. The energy of dissociation is much larger for regular systems than statistical. The dissociation for MCDEA cured elastomers occurs about 30°C higher than for Mboca cured elastomers (see Table III).
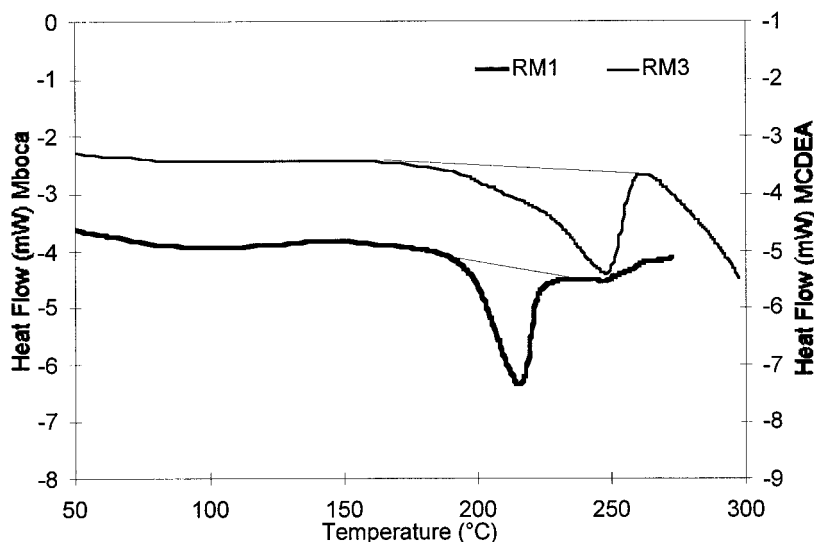
Figure 9. Comparison of the Mboca cured elastomer to MCDEA elastomer heat of dissociation and hard segment T_g. For Mboca cured elastomers, there is a drop in baseline suggesting T_g of hard segment occurs in same temperature range as dissociation, while for MCDEA cured elastomers, the baseline is level and a transition occurs immediately after the dissociation followed by degradation of the elastomer (see Table III).

determine the energy per mol of hard segment. The temperature of dissociation for the MCDEA elastomers is about 240°C compared to 210°C for the Mboca elastomers.

The glass-transition temperature for the hard domain was difficult to determine. For the Mboca elastomer series, it appears to be occurring in the same temperature range as the dissociation of the hydrogen bonding. The baseline is lower after the dissociation. For the MCDEA elastomer series, there appears to be a glass transition immediately following the dissociation. The baseline before and after the dissociation is constant (Fig. 9). When the elastomers are heated through the region, quenched, and then reheated there is a small glass transition occurring at 210°C for Mboca cured elastomers and one at 260°C for MCDEA cured elastomers. When running modulated DSC on these samples, there is a reversible and nonreversible transition in these temperature ranges (Fig. 10), interpreted as a nonreversible dissociation of the hydrogen bonding and a reversible glass-transition temperature.

Quantitatively, the mass fraction of hard segment mixed in the soft domains can be approximated by application of the Fox equation,[40]

$$\frac{1}{T_g} = \frac{w_1}{T_{g1}} + \frac{w_2}{T_{g2}} \qquad (6)$$

where w_1 is the mass fraction of the soft segment and w_2 is the mass fraction hard segment in the soft domains and $w_1 + w_2 = 1$. The T_g of pure PTMEG is approximately −85°C. The transition temperature is increased about 10°C because the chains are anchored at each end,[41] so that the glass-transition temperature for a pure PTMEG soft domain would be −75°C.[18]

The density of all of the polyurethanes studied was approximately 1.10 ∓ .002 g/cm³. As a zeroth approximation in the following, the densities of both the hard domains and the soft domains will be considered equal, even though the hard domains actually have slightly higher densities. The mass fraction of the hard segment in the soft domains was calculated using the DSC values for the average glass-transition temperatures for the hard and soft domains. For the Mboca cured elastomer, $w_1 = 0.85$. If the total mass of the material is divided into 100 parts then it can be assumed that 61 of those parts consist of PTMEG in the soft domains. However, this accounts for only 85% of the mass of the soft segments. The soft segment must therefore comprise 72 parts of the total (61/0.85). This means that 28 parts are pure hard segment (TDI/Mboca). The 11 parts not yet accounted for can be assigned to hard segment (TDI/Mboca) monomers dissolved in the soft domains. This is consistent with the value of 0.15 for w_2.
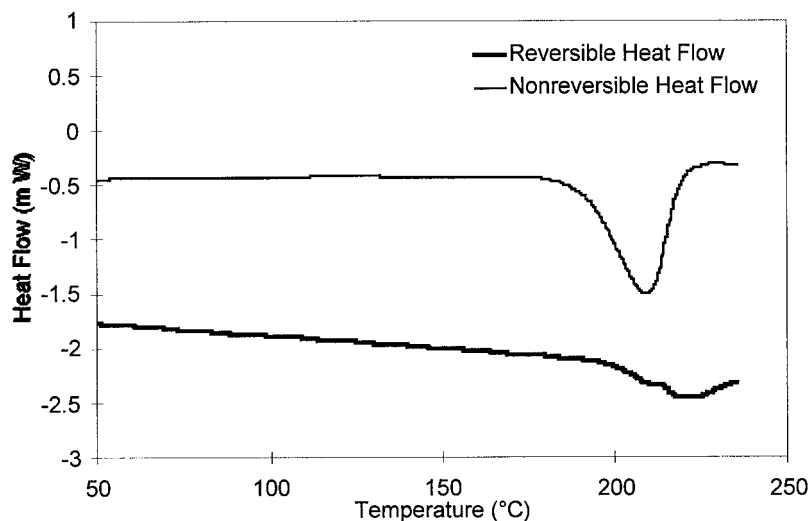
Figure 10. Modulated DSC scan of R(2,4/2,6) Mboca showing the reversible hard segment T_g and the nonreversible dissociation of the hydrogen bonding. The composite DSC scan is shown in Figure 9.

The mass fraction hard domains (V_h) for the Mboca cured elastomers is therefore about 0.28. Following the same procedure for the MCDEA cured elastomers, for which $w_1 = 0.92$, yields a value of 0.38 for V_h, with five parts of the hard segment dissolved in the soft domain.

SAXS

The important features of the SAXS data are shown in Figures 4 and 5. The distinctions between the R and S samples as well as the distinctions between treatments for the two series are evident. The data from the $q^2I(q)$ sets were converted into correlation functions using a program supplied by Dr. Richard Goddard. The error bars shown in the plots presented here are twice the standard deviations of the mean intensity values as computed for each value of q in the circular averaging process used to reduce the area detector data to tables of $I(q)$. For Figure 4, the relative error bars amount to less than 2% of the plotted value, so that their size is comparable to that of the plotting symbols for large values of q. In Figure 5, the error bars at large values of q are amplified by the factor of q^4 used to generate the transformation for viewing the Porod law behavior. The data in Figure 5 suggest that these systems obey Porod's law in an approximate sense. However, data is needed at larger values of q in order to assess departures from ideal Porod Law behavior.

A representative sample of the correlation functions derived from the data is shown in Figure 11. Table IV summarizes the morphology data derived from all of the SAXS and DSC experiments. The values in this table should be viewed as comparative estimates only. There are currently no standard methods for deriving confidence intervals for these parameters based on the noise in the experimental data. The analysis of data from replicate specimens for selected preparations show that the estimates are repeatable to within 5% of the mean for identically prepared samples within this series of data collection runs. Standard samples that might be used to judge the accuracy of distance estimates derived from correlation function analyses do not exist at this time.

The values for L_1 range from 7.6 nm to 4.5 nm. Within a curative set, the elastomers from the R prepolymers have a smaller value of L than the elastomers from the S prepolymers. The MCDEA cured elastomers have a smaller value of L than the Mboca cured elastomers from the same prepolymer. Additional annealing of the MCDEA elastomers appeared to have little effect on L. The long period estimators L_1 and L_2 show similar trends and their values are in excellent agreement, except in the case of specimen 1A. The breadth and the skewed character of the scattering peak for this sample suggest considerable randomness in the microstructure of this material.
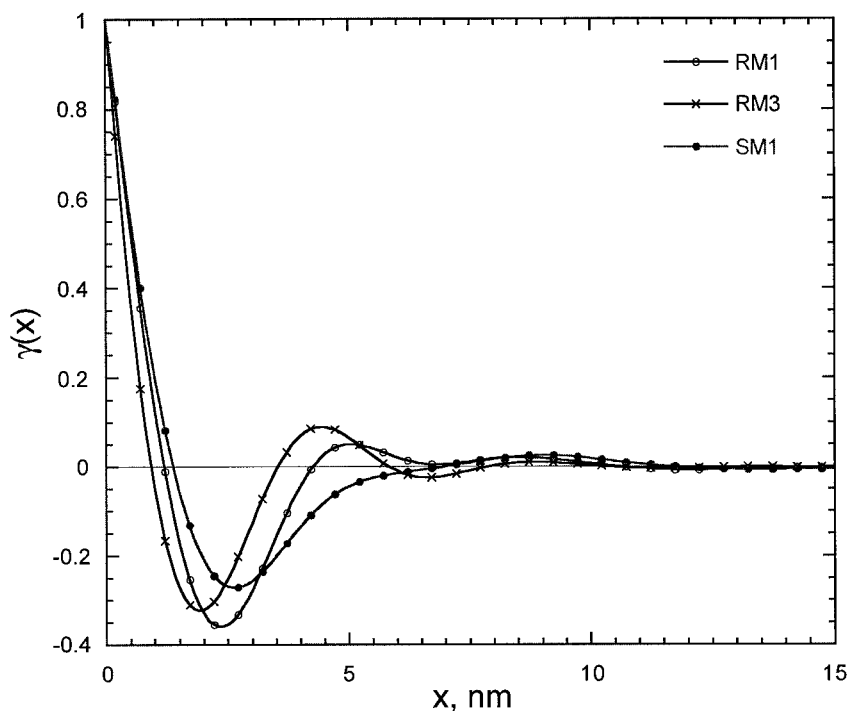
Figure 11. One-dimensional correlation functions for selected poly(urethaneurea) samples.

The hard domain thickness (H) can be determined from the one-dimensional correlation function or from the V_h determined by DSC and the $H(1-V_h)$ value from the correlation function. The values for H using either determination show that hard domain lamellae are thinner for elas-

Table IV. Morphology Data-SAXS and DSC Derived

| Sample ID (Table I) | Interdomain Spacing- L (nm) | | H (nm) | | A (nm)[d] | V_h | | K_p |
	Bragg[a]	1-D C.F.[b]	SAXS[b]	DSC[c]		DSC[e]	SAXS[f]	
SM1	7.6	9.2	1.78	1.94	7.42	0.28	0.22	0.86
SP1	6.8	7.0	1.72	1.87	5.28	0.28	0.23	0.93
RM1	5.1	5.0	1.61	1.69	3.39	0.28	0.25	1.11
RP1	5.2	5.2	1.64	1.69	3.56	0.28	0.27	1.01
SM2	5.3	5.2	1.47	1.84	3.73	0.38	0.24	1.02
SP2	5.2	4.9	1.38	1.69	3.52	0.38	0.25	0.98
RM2	4.5	4.5	1.22	1.51	3.28	0.38	0.25	1.51
RP2	4.5	4.5	1.28	1.59	3.22	0.38	0.24	1.35
SM3	5.2	5.7	1.31	1.67	4.39	0.38	0.22	0.77
SP3	5.1	5.2	1.30	1.64	3.90	0.38	0.24	1.02
RM3	4.5	4.5	1.19	1.47	3.31	0.38	0.24	1.39
RP3	4.5	4.5	1.18	1.49	3.32	0.38	0.23	1.25

[a] I_q^2 vs. q plot.
[b] 1-d correlation function.
[c] Correlation function modified by DSC-V_h (DSC) and H(1-V_h) (SAXS).
[d] $A = L - H$ from correlation function.
[e] DSC/Fox equation.
[f] Correlation function—$H(1 - V_h)$ and H.

tomers from the R prepolymers as compared with those from the S prepolymers. The MCDEA cured elastomers have even smaller hard segment thickness than Mboca cured elastomers and the longer cure at higher temperature leads to an even smaller hard segment thickness. Since the soft segment domain thickness, A, is obtained by subtracting H from L the values follow the same trend as H and L where the R elastomers cured with MCDEA have the smallest soft segment thickness.
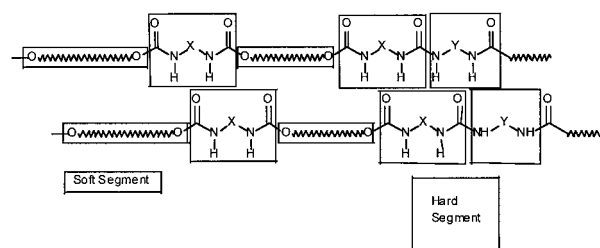
The V_h was determined from the one-dimensional correlation function and also from DSC by application of the Fox equation. The SAXS and DSC show a similar pattern, where the V_h is relatively constant within each curative set. The V_h for the MCDEA cured elastomers is, however, significantly lower for SAXS derived values than for the DSC values.

DISCUSSION

The data consistently show a difference between elastomers from the S prepolymers and the R prepolymers as well as differences between the MCDEA and Mboca chain extenders. The moduli and tensile strengths are higher for the R elastomers and the MCDEA cured elastomers. The DSC shows larger heats of dissociation for the R elastomers compared to the S elastomers. The MCDEA cured elastomers show lower soft segment T_g and higher dissociation temperatures for the hard segments than the Mboca cured elastomers. The SAXS data show the R elastomers to have smaller but better organized phase domains than the S elastomer.

When comparing the plots of $I(q)q^2$ vs. q (Fig. 4) the q_{max} values are larger (smaller L_1), the peak is much narrower, and the shape is more symmetrical for the elastomers from the R prepolymers as compared to elastomers from the S prepolymers within all cure conditions. Curing with MCDEA rather than with Mboca makes the peak shape even more symmetrical. These features suggest that domains are more ordered for the elastomers from the R prepolymers compared to the elastomers from the S prepolymers and that curing with MCDEA allows for even more regular, better ordered domains.

Figure 12 illustrates the positions of the hard and soft segments, and the sites for hydrogen bonding between the N–H moieties and the oxygens. A likely interpretation is that the more or-

X = Isocyanate- TDI
Y= Amine Curative- Mboca or MCDEA

Figure 12.   Model of alignment of hard segment to allow hydrogen bonding. In elastomers with a large percentage of high molecular weight oligomers, there are more hard segments without curative and the amount of hydrogen bonding is significantly decreased. When both X and Y are found in the hard segment, hydrogen bonding can occur.

dered elastomers from the R prepolymers have more sites for the hard segments to align, creating improved sites for hydrogen bonding. When there are higher molecular mass oligomers there are fewer locations for hydrogen bonding. The heat of dissociation is related to the hydrogen bonding between adjacent hard segments. The bond dissociation energy for a hydrogen bond is about 21 kJ/mol. The heat of dissociation for the S systems corresponds to about one hydrogen bond per mole of hard segment while the R systems have two to three hydrogen bonds per mole of hard segment. This increase in hydrogen bonding is presumably related to the increased order of the R- based materials. Thus, the DSC data show that elastomers from the R prepolymer have the same quantitative level of phase separation as the S elastomers but have better order, presumably due to more sites for hydrogen bonding. Similarly, the MCDEA elastomers have better phase separation than the Mboca elastomers.

A result of the better organization of the hard segment and the increased hydrogen bonding is the higher modulus of the elastomers from the R prepolymers as shown in Table II. The even better organization or regularity of the hard domains for the MCDEA cured elastomers results in elastomers with even higher modulus. The differences in tensile modulus between the R prepolymers and the S prepolymers cured with MCDEA appear to be less significant than for curing with Mboca. The difference between the interdomain spacings for the S and R prepolymers cured with Mboca is much larger and its effects are more obvious in the tensile modulus behavior.

The limiting power law behavior of the scattering data provides important insights into the character of the interfacial region. Porod's law predicts that the product of $I(q)q^4$ reaches a constant, K_p, as $q \rightarrow \infty$ for sharp boundaries in a two-phase material. When the data are plotted as in Figure 5, a positive slope in the high q region can be attributed to liquid-like scattering from the disordered material or phase mixing of the hard/soft segments. A negative slope indicates diffuseness in the boundaries between phases.[8,17,28,29,33–36] The plots in Figure 5 do not extend to large enough values of q to permit an estimate of either interfacial thickness or phase mixing based on deviations from Porod's Law. The values of K_p in Table IV are therefore to be taken as relative estimates only.

Tyagi et al.[34] and Ophir and Wilkes[17] state that comparisons of interfacial characteristics are most meaningful between materials of similar composition. In this case, within each curative set, the materials are the same, the only difference being the organization of prepolymer. The constant is related to the surface area to volume ratios of the microdomains.[9] Since the volume fraction of each phase is relatively constant as seen in DSC and SAXS data, differences in K_p must be attributed to differences in the surface area. The data for K_p as shown in Table IV show that elastomers from the R prepolymers have higher K_p values and therefore must have greater interfacial area. Since the sizes of the domains are smaller for the R elastomers, the greater interfacial area indicates that there may be more of the smaller domains. Figure 5 suggests a diminution of the interfacial specific surface area on annealing of the MCDEA cured materials.

CONCLUSIONS

The tensile moduli and other mechanical properties of the R elastomers were higher than those of the S elastomers. In addition, there were higher values overall for mechanical properties with MCDEA rather than Mboca as the curative. These improvements can be correlated with increased hydrogen bonding, smaller domains, and greater interfacial area.

For the prepolymers in this study, those with a more controlled, reduced molecular mass polydispersity are estimated to have two to three times more sites for hydrogen bonding of the hard domains, as shown by the larger heats of dissociation for the R elastomers. However, within a cur-

ative set there are no significant differences in T_g and dissociation temperatures, suggesting that the volume fraction of each phase is the same for the two types of prepolymers. However, the elastomers from the R prepolymers have better-organized phases due to increased hydrogen bonding. The DSC data also show a lower T_g and higher dissociation temperature for the MCDEA cured elastomers, indicating greater phase separation compared to the Mboca cured elastomers.

The SAXS data indicate that the volume fractions of each phase are constant within a curative set. The sizes of the phases, however, are significantly smaller for elastomers from the R prepolymers and even smaller when the prepolymers are cured with MCDEA. In addition, the Porod's constant K_p, a ratio of interface area to volume, shows that the R elastomers have greater interfacial area than the S elastomers, which suggests a larger number of smaller domains for the R elastomers.

The current results strongly suggest that an elastomer produced from a prepolymer with a narrower molecular mass polydispersity yields improved mechanical properties as a result of smaller, more ordered domains, and greater interfacial area. The domains are made still smaller and better organized by the use of MCDEA as a curative/chain extender, as compared to those prepared with Mboca.

REFERENCES AND NOTES

1. Odian, G. Principles of Polymerization; Wiley: New York, 1991; 3rd ed., Chapter 2.
2. Siuta, A. J.; Starner, W. E.; Toseland, B. A.; Machado, R. M. Preparation of Urethane Prepolymers Having Low Levels of Residual Toluene Diisocyante, U.S. Patent 5,051,152, Air Products and Chemicals, Inc., 1991.
3. Clift, S. M.; Clement, A. L.; Quay, J. R.; Dewhurst, J. E. Airthane High Performance Polyurethane Prepolymers, Air Products and Chemicals, Inc., 1992.
4. Starner, W. E.; Casey, J. P.; Miligan, B.; Clift, S. M. Process for the Preparation of Polyisocyanate Pre-

polymers and Polyurethanes Having High Temperature Performance and Low Hysterisis, U.S. Patent 4,786,703, Air Products and Chemicals, Inc., 1988.

5. McInnis, E. L. Optimization of High Performance Elastomer Properties, Air Products and Chemicals, Inc., 1994.

6. Ryan, A. J.; Naylor, S.; Komanschek, B.; Bras, W.; Mant, G. R.; Derbyshire, G. E. In Hyphenated Techniques in Polymer Characterization; Provder, T.; Urban, M. W.; Barth, H. G., Eds.; ACS Symposium Series No. 581, American Chemical Society: Washington, D.C., 1994.

7. Koberstein, J. T.; Stein, R. S. J Polym Sci: Polym Phys Ed 1983, 21, 2181.

8. Koberstein, J. T.; Stein, R. S. J Polym Sci: Polym Phys Ed 1983, 21, 1439.

9. Leung, L. M.; Koberstein, J. T. J Polym Sci Part B: Polym Phys Ed 1985, 23, 1883.

10. Leung, L. M.; Koberstein, J. T. Macromolecules 1986, 19,706.

11. Koberstein, J. T.; Yu, C. C.; Galambos, A. F.; Russell, T. P.; Ryan, A. J. Polym Prep 1990, 31(2), 10.

12. Koberstein, J. T.; Galambos, A. F. Macromolecules 1992, 25, 5618.

13. Koberstein, J. T.; Russell, T. P. Macromolecules 1986, 19, 714.

14. Chu, B.; Gao, T.; Li, Y.; Wang, J.; Desper, C. R.; Bryne, C. A. Macromolecules 1992, 25, 5724.

15. Martin, D. J.; Meijs, G. F.; Remwick, G. M.; Gunatillake, P. A.; McCarthy, S. J. J Appl Polym Sci 1996, 60, 557.

16. Martin, D. J.; Meijs, G. F.; Remwick, G. M.; McCarthy, S. J.; Gunatillake, P. A. J Appl Polym Sci 1996, 62, 1337.

17. Ophir, Z.; Wilkes, G. L. J Polym Sci: Polym Phys Ed 1980, 18, 1469.

18. Paik Sung, C. S.; Smith, T. W.; Sung, N. H. Macromolecules 1980, 13, 117.

19. Paik Sung, C. S.; Hu, C. B.; Wu, C. S. Macromolecules 1980, 13, 111.

20. Etienne, S.; Vigier, G.; Cuve, L.; Pascault, J. P. Polymer 1994, 35, 2737.

21. Li, Y.; Ren, Z.; Zhao, M.; Yang, H.; Chu, B. Macromolecules 1984, 17, 1063.

22. Marcos-Fernandez, A.; Ryan, A. J.; Gonzalez, L. Nucl Instr Meth Phys Res, Sect B 1995, 97, 279.

23. Linliu, K.; Chen, S. A.; Yu, T. L.; Lin, T. L.; Lee, C. H.; Kai, J. J.; Chang, S. L.; Lin, J. S. J Polym Res 1995, 2, 63.

24. Schneider, N. S.; Paik Sung, C. S.; Matton, R. W.; Illinger, J. L. Macromolecules 1975, 1, 62.

25. Song, Y. M.; Chen, W. C.; Yu, T. L.; Linliu, K.; Tseng, Y. H. J Appl Polym Sci 1996, 62, 827.

26. Guinier, A.; Fornet, G. Small-Angle Scattering of X-Rays; John Wiley and Sons: New York, 1955.

27. Feigin, L. A.; Svergun, D. I. Structure Analysis by Small-Angle X-Ray and Neutron Scattering; Plenum Press: New York, 1987.

28. Vonk, C. G.; Kortleve, G. Kolloid Z 1967, 220, 19.

29. Vonk, C. G. J Appl Cryst 1973, 6, 81.

30. Strobl, G. R.; Schneider, M. J. J Polym Sci: Polym Phys Ed 1980, 18, 1343.

31. Porod, G. Kolloid Z 1951,124, 83.

32. Porod, G. Kolloid Z 1952, 125, 51, 108.

33. Bonart, R.; Miller, E. H. J Macromol Sci Phys 1974, B10, 177.

34. Tyagi, D.; McGrath, J. E.; Wilkes, G. L. Polym Eng Sci 1986, 26, 1371.

35. Myers, E.; Wims, A. M.; Ellis, T. S.; Barnes, J. Macromolecules 1990, 23, 2807.

36. Goddard, R. J.; Cooper, S. L. J Polym Sci Part B: Polym Phys Ed 1994, 32, 1557.

37. Certain commercial equipment, instruments, or materials are identified in this paper in order to specify the experimental procedure adequately. Such identification is not intended to imply recommendation or endorsement by the National Institute of Standards and Technology, nor is it intended to imply that the materials or equipment identified are necessarily the best available for the purpose.

38. ASTM Annual Book of Standards; ASTM: Philadelphia, 1997; Vol. 09.01.

39. Hendricks, R. J Appl Cryst 1978, 11, 15.

40. Schneider, H. A.; DiMarzio, E. A. Polymer 1992, 33, 3453.

41. DiMarzio, E. A. J Res Natl Bur Stand 1964, 68A, 611.